Performance Evaluation of Peer-to-Peer Distributed Microgrids Coordination for Voltage Regulation

Preprint

Houchao Gan,[1,2] Jing Wang,[1] Yashen Lin,[1]
Siddharth Bhela,[3] and Chris Bilby[4]

1 National Renewable Energy Laboratory
2 Clarkson University
3 Siemens Technology
4 Holy Cross Energy

Presented at the 2022 IEEE Power and Energy Society General Meeting
Denver, Colorado
July 17–21, 2022

NREL is a national laboratory of the U.S. Department of Energy
Office of Energy Efficiency & Renewable Energy
Operated by the Alliance for Sustainable Energy, LLC

This report is available at no cost from the National Renewable Energy Laboratory (NREL) at www.nrel.gov/publications.

Contract No. DE-AC36-08GO28308

Conference Paper
NREL/CP-5D00-81427
July 2022

Performance Evaluation of Peer-to-Peer Distributed Microgrids Coordination for Voltage Regulation

Preprint

Houchao Gan,[1,2] Jing Wang,[1] Yashen Lin,[1]
Siddharth Bhela,[3] and Chris Bilby[4]

1 National Renewable Energy Laboratory
2 Clarkson University
3 Siemens Technology
4 Holy Cross Energy

Suggested Citation
Gan, Houchao, Jing Wang, Yashen Lin, Siddharth Bhela, and Chris Bilby. 2022. *Performance Evaluation of Peer-to-Peer Distributed Microgrids Coordination for Voltage Regulation: Preprint*. Golden, CO: National Renewable Energy Laboratory. NREL/CP-5D00-81427. https://www.nrel.gov/docs/fy22osti/81427.pdf.

NREL is a national laboratory of the U.S. Department of Energy
Office of Energy Efficiency & Renewable Energy
Operated by the Alliance for Sustainable Energy, LLC

This report is available at no cost from the National Renewable Energy Laboratory (NREL) at www.nrel.gov/publications.

Contract No. DE-AC36-08GO28308

Conference Paper
NREL/CP-5D00-81427
July 2022

National Renewable Energy Laboratory
15013 Denver West Parkway
Golden, CO 80401
303-275-3000 • www.nrel.gov

NOTICE

This work was authored in part by the National Renewable Energy Laboratory, operated by Alliance for Sustainable Energy, LLC, for the U.S. Department of Energy (DOE) under Contract No. DE-AC36-08GO28308. Funding provided by the U.S Department of Energy Office of Energy Efficiency and Renewable Energy Solar Energy Technologies Office under Award Number EE0008769. The views expressed herein do not necessarily represent the views of the DOE or the U.S. Government.

Cover Photos by Dennis Schroeder: (clockwise, left to right) NREL 51934, NREL 45897, NREL 42160, NREL 45891, NREL 48097, NREL 46526.

Performance Evaluation of Peer-to-Peer Distributed Microgrids Coordination for Voltage Regulation

Houchao Gan[1,2], Jing Wang[1], Yashen Lin[1], Siddharth Bhela[3], Chris Bilby[4]
[1]Power Systems Engineering Center, National Renewable Energy Laboratory, Golden, CO 80401, USA
[2]Electrical and Computer Engineering, Clarkson University, Potsdam, NY 13699, USA
[3]Siemens Technology, Princeton, NJ, USA
[4]Holy Cross Energy, 3799 Highway 82, Glenwood Springs, CO 81601
Jing.Wang@nrel.gov, Yashen.Lin@nrel.gov

***Abstract*— This paper presents the performance evaluation of a peer-to-peer microgrids coordination algorithm for sub-transmission systems. As distributed energy resources (DERs) in distribution system start to show negative impact to the bulk power system, a paradigm shift is needed for transmission planning and operation. Because distribution substations are located far from the sub-transmission system, and it is hard to use traditional centralized control for real-time control and coordination. Thus, distributed control is a natural choice because it requires less communication and central computation. In this paper, each distribution substation is treated as a microgrid, and the peer-to-peer distributed microgrids control is formulated as a real-time optimal power flow problem to reduce the negative impact in sub-transmission systems. A distributed primal-dual optimization algorithm is adopted to solve the problem. Validation of the peer-to-peer algorithm is performed through the simulation of a real-world sub-transmission system composing of many distribution systems with high renewable penetration. Simulation results show that the peer-to-peer algorithm can achieve satisfactory voltage regulation performance in sub-transmission system by coordinating and controlling DERs in distribution systems.**

***Index Terms*—Microgrid coordination, distributed control, HELICS, peer-to-peer control algorithm, voltage regulation.**

I. INTRODUCTION

The increasing penetration of distributed energy resources (DERs) in distribution systems has created new challenges and opportunities in power systems. Although most DERs are connected to the distribution systems, their impacts could reach sub-transmission and transmission systems, creating challenges such as intermittent power generation, stochastic operating conditions, and reverse power flow [1]. This requires transmission system planners and operators to explore grid operation and control solutions to maintain transmission system stability and to cope with the ever-increasing integration of DERs [2]. The grid operation and control solutions usually require coordination and control between transmission and distribution systems, which imposes challenges for control systems, especially communication networks, because distribution substations are located far from the sub-transmission system, and it is hard to use traditional centralized control for real-time control and coordination [3].

Distributed control architecture is a promising option to achieve this goal of coordinating DERs for maintaining reliable operation of sub-transmission systems. It does not require a central controller; local controllers exchange information with neighbors to achieve network level objectives [4]. Due to these advantages, distributed DER control and coordination has received attentions in many studies, for example, [5-6]. However, they are mostly considered in the distribution system context. Grid control solution for DERs at the sub-transmission and transmission level, which includes many distribution systems, is not well studied. To bridge this gap, this paper aims to develop a distributed control framework for microgrids coordination that enables neighboring distribution substations to share information and help each other for system level objectives (e.g., voltage regulation), while reducing the need for communication in the system.

The main contributions of this paper are as follows: i) A distributed control framework is applied to coordinate distribution substations as microgrids to achieve network-level objectives while maintaining system constraints. ii) The peer-to-peer control algorithm is tested with a real-world sub-transmission system; detailed design, implementation, and tuning of the algorithm are provided; and the case study provides insights into how a distribution system with a high penetration of renewable generation impacts the sub-transmission system and demonstrates the ability of DERs in distribution systems to maintain sub-transmission system voltage stability through distributed controls. iii) Two communication scenarios—all-to-all and neighbor-to-neighbor—are investigated, and the results show that the neighbor-to-neighbor communication has similar control performance to the all-to-all communication but with less need for communication networks.

II. PEER-TO-PEER ALGORITHM DESCRIPTION

A. Problem Formulation

We consider a power system of N nodes, which is divided into N_{MG} microgrids. Each microgrid has a microgrid controller (MGC), which controls the local DERs, collects local measurements, and communicates with other MGCs. Our objective is to coordinate the microgrids in a distributed fashion while achieving certain network objectives and satisfying system constraints. The generic optimal power flow (OPF) problem can be formulated as follows:

$$\min_{x} \sum_{k=1}^{N} f_k(\boldsymbol{x}_k) \qquad (1a)$$

$$s.t. \quad Power\ flow\ equations \qquad (1b)$$

This work was authored in part by the National Renewable Energy Laboratory, operated by Alliance for Sustainable Energy, LLC, for the U.S. Department of Energy (DOE) under Contract No. DE-AC36-08GO28308. Funding provided by the U.S Department of Energy Office of Energy Efficiency and Renewable Energy Solar Energy Technologies Office under Award Number DE-EE0008769. The views expressed in the article do not necessarily represent the views of the DOE or the U.S. Government. The U.S. Government retains and the publisher, by accepting the article for publication, acknowledges that the U.S. Government retains a nonexclusive, paid-up, irrevocable, worldwide license to publish or reproduce the published form of this work, or allow others to do so, for U.S. Government purposes.

$$Voltage\ limits \quad (1c)$$
$$Device\ limits \quad (1d)$$

where x are the decision variables; $f(\cdot)$ are the objective functions. Note that the formulation in (1) is generic; the choice of decision variables, objectives, and constraints depends on the specific interests of the user. Different choice also leads to different level of complexity and requires different algorithm to solve. In this work, x are chosen to be the real and reactive power of the controllable DERs; the objective is to minimize real power curtailment and reactive power injection; a linearized power flow from [7] is adopted for constraint (1b); lower and upper bounds are set for (1c); and upper bounds for the apparent power of the DERs are set for (1d).

B. Peer-to-Peer Algorithm

To solve the OPF in peer-to-peer fashion, we adopted a distributed primal-dual gradient algorithm from [9]. In the standard primal-dual algorithm, global information of the dual variable is needed, making it a centralized algorithm [8]. In the distributed algorithm, each MGC keeps a local estimate of the dual variables, $\hat{\lambda}_k$. The dual estimates are updated with local measurements and communication with the other MGCs, resulting in a fully distributed algorithm. Also, the algorithm uses real-time measurements to update the optimization iterations, which reduces the impacts of modeling errors and computation costs [7].

The primal variable update is given by the following: let $\mathcal{N}_D$ be the set of indexes for controllable DERs, $\forall k \in \mathcal{N}_D$:

$$x_{k,t+1} = \text{Proj}_{\mathcal{X}}\left[x_{k,t} + \alpha\left(\nabla f_k(x_{k,t}) + A_k\hat{\lambda}_{k,t}\right)\right] \quad (2)$$

and the dual variable estimate update is given by the following: let $\mathcal{N}_v$ be the set of indexes for the constraints, $\forall j \in \mathcal{N}_v$:

$$\hat{\lambda}_{j,t+1} = \text{Proj}_{\mathbb{R}^+}\left[\hat{\lambda}_{j,t} + \beta M\left(y_{j,t} - b_j\right)\right] - \gamma L\hat{\lambda}_{j,t} \quad (3)$$

where $\text{Proj}_{\mathcal{S}}[\circ]$ is the projection operator which finds the closest point to the operand in the set $\mathcal{S}$; A_k is calculated from the linearized power flow equation; $\hat{\boldsymbol{\lambda}}_j$ collects all the copies of estimate for the j^{th} constraint; y and b are the voltage measurements and the corresponding voltage limits; α, β, γ are the step sizes for the primal variable update, dual variable estimate update, and communications, which can be tuned to ensure convergence and improve the algorithm's performance; M is a connection matrix specifying which measurements each MGC has; and L is the graph Laplacian of the communication graph.

At each time step, the MGC will (i) update the primal variables with the local estimate of the dual variables according to (2) and (ii) collect local measurements of the constraints and dual variable estimates from other MGCs and update its local dual variable estimate following (3). More analysis on the algorithm can be found in [9].

III. Description of the Evaluation Setup

This work validates the performance of the peer-to-peer control algorithm under a simulated real-world sub-transmission system of Holy Cross Energy (HCE), a local utility company in Colorado. When distribution systems have large amounts of renewable generation, reverse power flow might occur, which could lead to voltage issues in the sub-transmission systems. In this study, we aim to optimize DER operations while ensuring voltage constraints are satisfied.

Fig. 1 shows the overall diagram of the peer-to-peer evaluation setup. The sub-transmission system model is simulated in OpenDSS and measurements and control setpoints are exchanged with MGCs; the MGC is the distributed microgrid controller; and the data manager is to simulate the communication between MGCs. All the elements are implemented in the Hierarchical Engine for Large-scale Infrastructure Co-Simulation (HELICS) platform. HELICS is used because it allows each main element to execute in its own time step in real time, and it allows for real-time data exchange between elements, which is important for testing real-time controls interacting with the simulation model [10]. The following subsections explain each main component in detail.

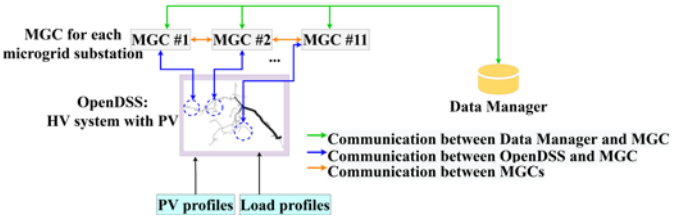

Fig. 1. Overall diagram of the HELICS platform for the peer-to-peer algorithm performance evaluation.

A. Simulation of Sub-transmission System in OpenDSS

The topology of the sub-transmission system under study is shown in Fig. 2. The system is simplified with lumped loads and DERs while still retaining the network topology, generation, and demand to accurately represent the real-world HCE sub-transmission system. The system has 84 three-phase nodes and a peak load of 249.86 MW. Note that T1, T2, and T3 are three nodes connecting to upstream transmission systems. T2 and T3 are modeled as generators to allow the power flow to converge. There are 11 substations, and each substation is considered as a microgrid with controllable nodes. Each node has both load and photovoltaics (PV) connected. The PV generation at each node is set to meet half of the peak load. Hourly load profiles for a year are obtained from the utility supervisory control and data acquisition (SCADA) system at HCE. The PV profiles are calculated based on the net profile from the advanced metering infrastructure and the load profiles, and the solar irradiance data are interpolated into 1-minute resolution.

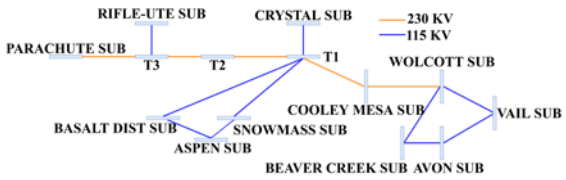

Fig. 2. Topology of the sub-tranmission system under study.

B. Peer-to-Peer Control Architecture

A high-level representation of the algorithm for each MGC is shown in Fig. 3. Following the algorithm described in Section II-B, each MGC updates the primal and dual variables locally with local measurements and dual variable estimates by communicating with other MGCs.

In this case study, the primal variables are a collection of the power set points $\boldsymbol{x} = [P_1, P_2 \ldots, P_n, Q_1, Q_2 \ldots Q_n]^T$ for all PV, which are dispatched by an MGC. The objective function is set to minimize the real power curtailment and the reactive power injection from the PV, i.e., $f(P_i, Q_i) = c_p\left(P_{av,i} - P_i\right)^2 + c_q(Q_i)^2$, where $P_{av,i}$ is the available active power for the i^{th} PV, and c_p and c_q are the weighting factors for the real and the reactive power costs. Note that, as shown in (3),

updating the estimation of the dual variable, $\hat{\lambda}$, includes two parts: $\beta M(y-b)$ and $\gamma L\hat{\lambda}$. The first part relates to constraint violation, where a voltage violation vector, V_{iol}, is defined as $V_{iol} = [V_{iol\_max},\ V_{iol\_min}]^T$, where $V_{iol\_max} = V_{mea} - V_{max}$ and $V_{iol\_min} = V_{mea} - V_{min}$ are defined to capture the difference between the voltage measurements, V_{mea}, and the target operation limit. Next, $\beta M V_{iol}$ is calculated. The second part of the dual variable update is calculated based on $\gamma L\hat{\lambda}$, where $\hat{\lambda}$ includes the estimated dual variables collected from the other MGCs. Note that the first term is related to local control, and the second term is related to communications with other MGCs control. If a voltage violation happens in one MGC, the peer-to-peer algorithm will control both the local PV and PV from neighboring MGCs to contribute to the voltage regulation. This is a great advantage of the peer-to-peer control algorithm.

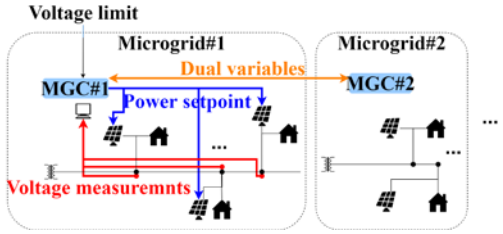

Fig. 3. Peer-to-peer algorithm for dispatching distributed PV.

C. Data Manager

In this primal and dual optimization scheme, each MGC needs to update its local dual variable estimate by requesting dual variables from other MGCs. A data manager as seen from Fig. 1 is implemented in HELICS as a storage to receive dual variables from all MGCs and to send the needed dual variables to the corresponding MGC. Note that the data manager is added to the simulation only for the convenience of communication implementation and it does not change the distributed nature of the algorithm; in practice, the data are exchanged in peer-to-peer fashion without centralized data management. When an MGC updates its dual variable estimate, the controller requests the data manager to send dual variables from the connected MGCs. The data manager processes this request and searches through the graph Laplacian L (communication graph among MGCs) to find the connected MGCs and collect the dual variables. The data manager then sends updated dual variables back to the MGC.

IV. Implementation of the Peer-to-Peer Algorithm

Defining the graph Laplacian L is the first step to implement the peer-to-peer algorithm. The sub-transmission system is divided into 11 zones based on the number of substations and interconnections, and each MGC controls all the PV units in that zone. The zone definitions are shown in Fig. 4. Zone 0 and 10 include one substation and transmission system(s), and the rest of the zones have only one substation.

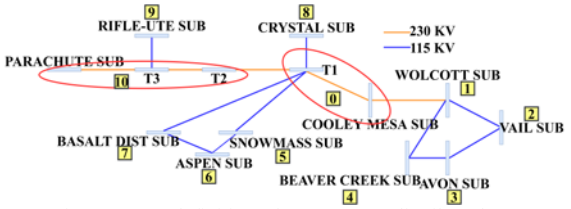

Fig. 4. Zone definition of peer-to-peer distributed MGCs.

The main function of the graph Laplacian L is to describe the communications between MGCs. In this work, we consider two types of communications: neighbor-to-neighbor and all-to-all. In the neighbor-to-neighbor communication, the MGC communicates with neighboring MGCs; and in the all-to-all communication, the MGC communicates with all other MGCs in the network. For example, Zone 0 connects with zones 1, 5, 7, 8, and 10, so the neighbor-to-neighbor communication of Zone 0 is described by the graph Laplacian L shown in Table 1.

Table 1. Graph Laplacian for neighbor-to-neighbor communication

	Z0	Z1	Z2	Z3	Z4	Z 5	Z 6	Z7	Z8	Z9	Z10
Z0	5	-1	0	0	0	-1	0	-1	-1	0	-1
⋮	⋮	⋮	⋮	⋮	⋮	⋮	⋮	⋮	⋮	⋮	⋮
Z10	-1	0	0	0	0	0	0	0	0	-1	2

For the all-to-all communication, the graph Laplacian L of Zone 0 is defined as shown in Table 2.

Table 2. Graph Laplacian for all-to-all communication

	Z0	Z1	Z2	Z3	Z4	Z 5	Z 6	Z7	Z8	Z9	Z10
Z0	10	-1	-1	-1	-1	-1	-1	-1	-1	-1	-1
⋮	⋮	⋮	⋮	⋮	⋮	⋮	⋮	⋮	⋮	⋮	⋮
Z10	-1	-1	-1	-1	-1	-1	-1	-1	-1	-1	10

After setting up the L, the peer-to-peer controller agents are configured in the HELICS framework. Fig. 5 presents a high-level structure of HELICS framework. Three types of agents are included in the framework: the OpenDSS agent, the MGC agents, and the data manager agent. For real-time simulation, the data manager agent runs every 0.1 second, the OpenDSS agent runs every 1 second, and the MGC agents run every 1 second. All the agents use HELICS's built-in publishing and subscription function to exchange data. As shown in Fig. 5, each MGC agent receives voltage measurements belonging to its zone from the OpenDSS agent, it also receives the requested dual variables from other MGCs, and the optimal P and Q set points are then sent to the OpenDSS agent. The data manager agent receives the dual variables from all the MGC agents and sends the requested dual variables to the corresponding MGC agents. Python is the programming language in HELICS and more details of the HELICS implementation can be found in reference [10].

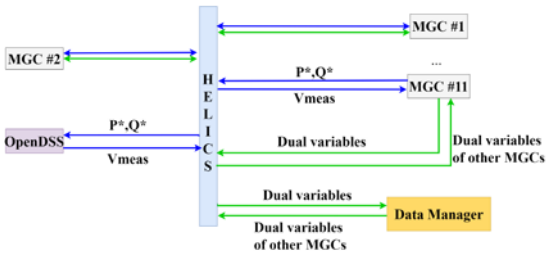

Fig. 5. HELICS framework of the peer-to-peer algorithm.

Once all the agents are integrated, a communication test is performed to ensure that the data are correctly transferred between agents. Then, a significant effort is spent on tuning the algorithm. The tunable variables include α and β, with α, β set to 0.1 as a starting point. The goals of the parameter tuning are to ensure that the algorithm converges and to find a good response speed (e.g., reactive power of PV and system voltages). Starting from 0.01 for both α and β, the reactive power outputs of the PV units are stable, but the system voltages are regulated very slowly, which indicates that the step size is too small. The values of α and β are gradually increased until the system voltages and reactive power output of the PV units start to oscillate when $\alpha = \beta = 1.8$. Between 0.01 and 1.8, different values of α, β are tested. If both α and β range from 0.01–1, the algorithm achieves a relatively

acceptable convergence time and voltage regulation performance. Finally, α and β are set to 0.05 to balance the convergence time and performance of the algorithm.

Y-matrix validation is another important aspect to ensure that the algorithm works correctly. Following [7], the coefficients in the linearized power flow constraint (1b) are calculated from the Y-matrix. The Y matrix is extracted from OpenDSS by disabling all voltage sources, PV units, and loads; then it is per-unitized. To have a sanity check on Y, we calculated the nominal voltage v_0 from Y and compare it with the voltage at the secondary of the transformer T1. The validation result shows that v_0 is very close to 1.04 p.u., with an acceptable error of 0.02%, indicating an accurate Y-matrix. Finally, the real-time simulation is performed to evaluate the voltage regulation performance against the target voltage operation limits and to ensure that the sub-transmission system model is stable with the applied power set points from the MGCs.

V. Simulation Results

This section presents the real-time simulation results to demonstrate the performance of the peer-to-peer control algorithm. In particular, the performances of the all-to-all and neighbor-to-neighbor communications are evaluated, and the differences between them are compared. For the evaluation, we select a 4-hour simulation window from 11:00 a.m.–15:00 p.m. to capture voltage issues that might result from large injections from PVs. Note that the power generated by PVs is approximately half of the active power demand. For comparison, we simulate a baseline scenario with PVs working in unity power factor control mode and there is no control actions for the system.

System Voltages: Fig. 6 shows the system voltages (maximum, average, and minimum) of the baseline scenario together with two communication scenarios. Note that in the baseline case, the voltages are within the common safe operation range (0.95 p.u.–1.05 p.u.); thus, for demonstration in this simulation, the lower and upper voltage limits are set to 0.95 p.u. and 1.038 p.u. to test the voltage regulation of the peer-to-peer algorithm. Compared to the baseline scenario, the system voltages with peer-to-peer control (all-to-all and neighbor-to-neighbor) show the regulation effect with the maximal voltage, and the average and minimal voltages are similar to the baseline scenario. Note that the voltage regulation performances of the two scenarios (all-to-all and neighbor-to-neighbor) resemble each other. Both scenarios cannot regulate the maximal voltage below the upper limit because the sub-transmission system is a very stiff grid, and the installed PV capacity might not have sufficient influence on the node with the maximal system voltage.

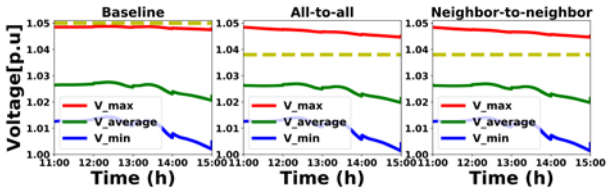

(a) (b) (c)

Fig. 6. System voltage measurements: (a) baseline (b) all-to-all communications, and (c) neighbor-to-neighbor communications.

Voltages of Two Selected Buses with High Voltages: Two buses, Bus R421B from Zone 9 and Bus BA411 from Zone 7, are selected because the voltages of these two zones violated the upper voltage limit, 1.038 p.u. The voltages of these two buses under three scenarios (baseline, all-to-all, and neighbor-to-neighbor) are presented in Fig. 7. Both control scenarios show the two buses being regulated compared to the voltage under the baseline scenario. Bus voltage V_R421B is still above the upper limit, whereas bus voltage V_BA411 is regulated within the limit. This is because the location of R421B is close to T2, which in the model is a big generator, and BA411 is downstream from the slack bus, T1. Note that BA411 is regulated within the limits in 10 minutes. Using the neighbor-to-neighbor communication, BA411 is regulated within the limits in 19 minutes. This shows that the peer-to-peer control algorithm takes longer to converge under the neighbor-to-neighbor communication.

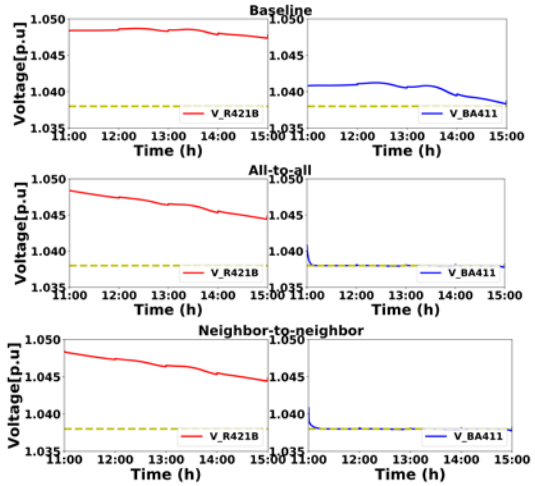

Fig. 7. Voltage measurements of buses: R421 (left) and BA411 (right).

Outputs of PVs of Two Selected Buses: Further demonstrating the peer-to-peer algorithm, the active and reactive power of the PV connected to two buses mentioned above are shown in Fig. 8 and Fig. 9, respectively. As shown in Fig. 8, PV at R421B has a large amount of active power curtailment (>30%) compared to the PV at BA411 (0.21%) for two scenarios. The curtailment of R421B keeps increasing because the measured voltage at R421B continuously violates the upper voltage limit. While BA411 can closely regulate its voltage without reducing active power.

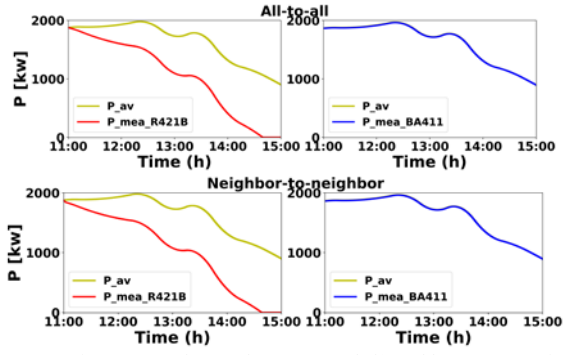

Fig. 8. Active power of PV at bus R421B (left) and bus BA411 (right).

As for the reactive power, the PV at R412B keeps increasing its reactive power output, and it stops at 4.192 MVar (near its capacity) for both communication scenarios. The PV at BA411 shows more dynamics in reactive power output, and it keeps increasing to certain value and then decreases to a near-zero value. The responses of the PV units at these two buses are expected because the peer-to-peer algorithm outputs reactive power as a priority and then curtails active power for voltage regulation.

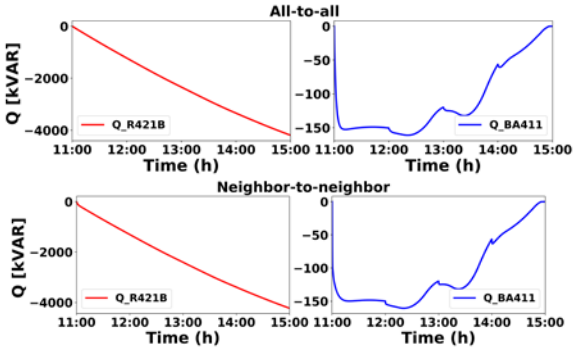

Fig. 9. Ractive power of the PV at R421B (left) and BA411 (right).

Dual Variables of PVs Connected to the Two Selected Buses: To further show the voltage regulation performance, dual variables (λ) related to the upper voltage violation are presented in Fig. 10. Each PV unit under one MGC receives the dual variables from peer MGCs. The dual variables of the PV at bus R421B keep increasing, as expected. The dual variables of PV at bus BA411 increase to their maximal, then start to decrease when bus BA411's voltage is below the upper voltage limit, and finally reduce to zero. Compared to the all-to-all scenario, the neighbor-to-neighbor scenario takes 14 minutes longer to reach zero. We can also see that the higher the overvoltage violation, the larger the dual variables. The results in Fig. 10 indicate that the dual variables respond correctly and dynamically to the system voltages; and as shown in Fig. 9.

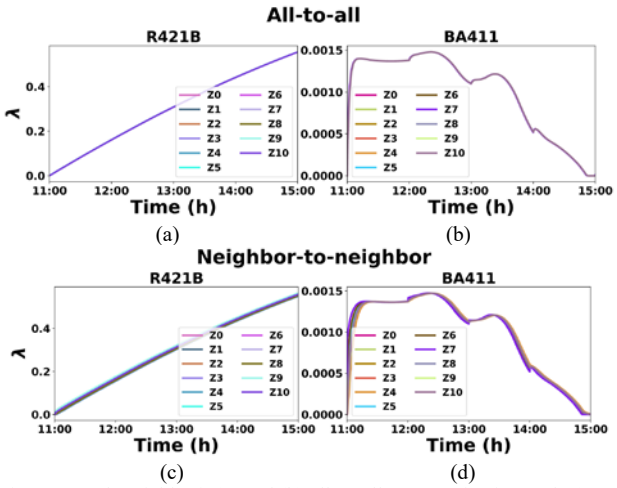

Fig. 10. Dual variables λ (a) and (b) all-to-all communication and (c) and (d) neighbor-to-neighbor communication.

Voltage Regulation Support from Neighboring MGCs: To investigate the contribution of the neighboring MGC to the voltage regulation at bus BA411, Fig. 11(a) presents the voltages of three buses that are selected from neighboring microgrids: ASPEN, SNOWMASS, and CRYSTAL. The voltage measurements of these buses are below the upper voltage limit, which requires no voltage regulation action. Fig. 11(b), however, shows that the PV at each bus absorbs a small amount of reactive power, which means that the neighboring microgrids contribute slightly to the voltage regulation at BA411. This further coincides with the mechanism of the peer-to-peer algorithm that the MGC shall contribute voltage regulation to interconnected peer MGCs.

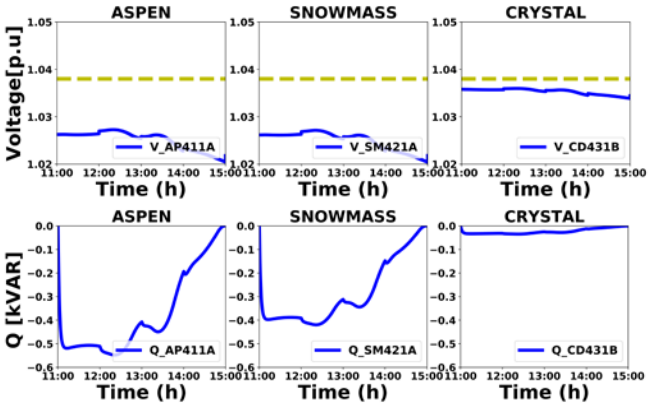

Fig. 11. Measurements of neighboring microgrids: voltage measurement (top) and reactive power output (bottom).

VI. Conclusions

This paper presented a distributed control algorithm for coordinating microgrids in sub-transmission systems with reduced need for communication. The algorithm was tested with a realistic sub-transmission system. The implementation of the control algorithm and simulation model is carried out through HELICS to ensure that the power system model and the distributed controllers run in real time. The detailed implementation and tuning of the peer-to-peer algorithm were described. Finally, the voltage regulation performance with two communication scenarios, all-to-all and neighbor-to-neighbor, were evaluated with 4-hour simulation of high solar production. The results demonstrate that (i) the peer-to-peer algorithm can regulate voltages of a sub-transmission system using aggregated DERs in distribution systems and the performance can be limited by a stiff power system and limited DER capacities, and (ii) the neighbor-to-neighbor communication has comparable control performance to the all-to-all scenario and requires less communications. We will investigate the peer-to-peer algorithm with asynchronous commutation in the future work.

References

[1] Technical Report, Impact of Distributed Energy Resources on the Bulk Electric System, ANL/ESD-17/26, Nov. 217.

[2] J. Zhao, J. Foster, Z. Dong, and K. Wong, "Flexible Transmission Network Planning Considering Distributed Generation Impacts," *IEEE Tran. Power Syst*., vol. 26, no. 3, Aug. 2011, pp. 1434-1443.

[3] IRENA, Co-operation Between Transmission and Distribution System Operators, ISBN 978-92-9260-178-2, 2020.

[4] D. E. Olivares, et al., "Trends in microgrid control," *IEEE Trans. Smart Grid*, vol. 5, no. 4, Jul. 2014, pp. 1905–1919.

[5] M. Tucci, et al., "A decentralized scalable approach to voltage control of DC islanded microgrids," *IEEE Trans. Control Syst. Technol*., vol. 24, no. 6, pp. 1965–1979, Nov. 2016

[6] C. Wei, et al., "An Optimal Scheduling Strategy for Peer-to-Peer Trading In Interconnected Microgrids Based on RO and Nash Bargaining," *Applied Energy*, 395 (2021) 117.24.

[7] S. Dhople, S. Guggilam, and Y. Chen. "Linear approximations to AC power flow in rectangular coordinates," *In 2015 53rd Annual Allerton Conference on Communication, Control, and Computing (Allerton)*, pp. 211-217. IEEE, 2015.

[8] D. K. Molzahn, et al., "A survey of distributed optimization and control algorithms for electric power systems," *IEEE Transactions on Smart Grid*, vol. 8, no. 6, Nov. 2017, pp.2941-2962.

[9] C. Chang, M. Colombino, J. Corte, and E. Dall'Anese, "Saddle-Flow Dynamics for Distributed Feedback-Based Optimization," *IEEE Control Systems Letters*, vol. 3, no. 4, Oct. 2019, pp.948-953.

[10] J. Wang, et al., "Performance Evaluation of Distributed Energy Resource Management via Advanced Hardware-in-the-Loop Simulation," *IEEE Power & Energy Society Innovative Smart Grid Technologies Conference (ISGT)*, Washington DC, 2020, pp.1-5.